

Journal of Materials Chemistry A

Accepted Manuscript



This is an *Accepted Manuscript*, which has been through the Royal Society of Chemistry peer review process and has been accepted for publication.

Accepted Manuscripts are published online shortly after acceptance, before technical editing, formatting and proof reading. Using this free service, authors can make their results available to the community, in citable form, before we publish the edited article. We will replace this *Accepted Manuscript* with the edited and formatted *Advance Article* as soon as it is available.

You can find more information about *Accepted Manuscripts* in the [Information for Authors](#).

Please note that technical editing may introduce minor changes to the text and/or graphics, which may alter content. The journal's standard [Terms & Conditions](#) and the [Ethical guidelines](#) still apply. In no event shall the Royal Society of Chemistry be held responsible for any errors or omissions in this *Accepted Manuscript* or any consequences arising from the use of any information it contains.



Journal Name

ARTICLE

Optimised room temperature, water-based synthesis of CPO-27-M metal-organic frameworks with high space-time yields †

L. Garzón-Tovar,^a A. Carné-Sánchez,^a C. Carbonell,^a I. Imaz^{a*} and D. MasPOCH^{ab*}Received 00th January 20xx,
Accepted 00th January 20xx

DOI: 10.1039/x0xx00000x

www.rsc.org/

The exceptional porosity of Metal-Organic Frameworks (MOFs) could be harnessed for countless practical applications. However, one of the challenges currently precluding the industrial exploitation of these materials is a lack of green methods for their synthesis. Since green synthetic methods obviate the use of organic solvents, they are expected to reduce the production costs, safety hazards and environmental impact typically associated with MOF fabrication. Herein we describe the stepwise optimisation of reaction parameters (pH, reagent concentrations and reaction time) for the room temperature, water-based synthesis of several members of the CPO-27/MOF-74-M series of MOFs, including ones made from Mg(II), Ni(II), Co(II) and Zn(II) ions. Using this method, we built MOFs with excellent BET surface areas and unprecedented Space-Time Yields (STYs). Employing this approach, we have synthesised CPO-27-M MOFs with record BET surface areas, including 1279 m² g⁻¹ (CPO-27-Zn), 1351 m² g⁻¹ (CPO-27-Ni), 1572 m² g⁻¹ (CPO-27-Co), and 1603 m² g⁻¹ (CPO-27-Mg). We anticipate that our method could be applied to produce CPO-27-Ni, -Mg, -Co and -Zn with STYs of 44 Kg m⁻³ day⁻¹, 191 Kg m⁻³ day⁻¹, 1462 Kg m⁻³ day⁻¹ and a record 18720 Kg m⁻³ day⁻¹, respectively.

Introduction

Metal-Organic Frameworks (MOFs) are an emerging class of porous materials comprising metal components and organic ligands. They are characterised by extremely large surface areas (S_{BET}) and high structural/compositional flexibility that confer them with potential for myriad applications, including gas sorption and separation, catalysis, sensing, and biomedicine, among many others.¹⁻⁷ Seeking to exploit this exceptional porosity, researchers have developed several methods for the industrial-scale fabrication of MOFs, including the classical solvothermal synthesis,⁸ mechano-synthesis,⁹ electrochemistry,¹⁰ continuous flow techniques,^{11,12} and spray-drying.¹³ These methods are continuously being optimised in the hopes of finally enabling widespread use of MOFs in practical applications.

Optimisation of industrial MOF fabrication methods not only addresses the production rates, but also the related costs, safety hazards and environmental impact. One measure that can simultaneously provide savings while improving safety and environmental friendliness is to use water as the only solvent. Along these lines, the company BASF has developed a water-based synthesis of aluminium fumarate (Basolite A520[®]) at the

tonne scale, achieving the extremely high Space-Time Yield (STY) of 3600 Kg m⁻³ day⁻¹.¹⁴ In fact, this breakthrough in the green synthesis of MOFs was awarded the Pierre Potier Prize.

Herein, we report another example of the green synthesis of MOFs: a room temperature, water-based synthesis of several members of the isostructural CPO-27-M (also known as *MOF-74*) family of the general structure $M_2(\text{dhtp})$, where dhtp = 2,5-dioxido-1,4-benzenedicarboxylate and M = Mg(II), Co(II), Ni(II) and Zn(II)] family at room temperature in terms of their production rates (STYs up to 18500 Kg m⁻³ day⁻¹) while maintaining their excellent sorption capabilities.

Isostructural CPO-27-M MOFs are undoubtedly among the most widely studied MOFs, as they are highly porous ($S_{\text{BET}} = 1039\text{-}1542 \text{ m}^2 \text{ g}^{-1}$) and stable and show hexagonal channels that can exhibit open metal sites and that can be easily functionalised with various groups.^{15, 16} Given these advantages, CPO-27-M MOFs are excellent candidates for catalysis,¹⁷ storage and delivery of biologically relevant gases,¹⁸ and separation and/or adsorption of gases (H₂, CO, CH₄, ammonia, etc.).¹⁹⁻²⁷ For instance, CPO-27-Mg has been widely reported to be among the best porous materials for CO₂ adsorption and separation due to its high selectivity, facile regeneration and high CO₂ dynamic-adsorption capacities.²⁸⁻³³

To date, the most common CPO-27-M syntheses involve solvothermal reactions of a solution containing the corresponding metal salt and dhtp in organic solvents (e.g. DMF) or mixtures of organic solvents and water.³⁴⁻³⁷ However, very recent reports have shown that totally water-based routes for the synthesis of CPO-27-M are possible and that, despite the low aqueous solubility of dhtp, such methods can be efficient. Quadrelli *et al.* first reported the synthesis of CPO-

^a ICN2 (ICN-CSIC), Institut Català de Nanociència i Nanotecnologia, Esfera UAB 08193 Bellaterra, Spain. E-mail: inhar.imaz@icn.cat; daniel.masPOCH@icn.cat.

^b Institució Catalana de Recerca i Estudis Avançats (ICREA), 08100 Barcelona, Spain

† Electronic Supplementary Information (ESI) available: [XRD patterns of the CPO-27-M series obtained with different reaction times and concentration. Tables listing the yield, S_{BET} values and synthesis conditions of CPO-27-M. XRD pattern and N₂ isotherm for the synthesis of CPO-27-Zn at gram scale. SEM images of CPO-27-M series]. See DOI: 10.1039/x0xx00000x

27-Ni ($S_{\text{BET}} = 1233 \text{ m}^2 \text{ g}^{-1}$) with an STY of $680 \text{ kg m}^{-3} \text{ day}^{-1}$. They mixed an aqueous solution of Ni(II) acetate with an aqueous suspension of dhtp, and then heated the resulting mixture at reflux for 1 h.³⁸ Their success stems from the use of Ni(II) acetate because metal acetates in the MOF syntheses can be used as both the metal source and the base (acetate ion).³⁹ Thus, the basic character of the acetate ion promotes deprotonation of the dhtp and therefore, its dissolution in water and subsequent reaction with Ni(II) ions. More recently, Sánchez-Sánchez *et al.* adapted this method to synthesise CPO-27-Zn ($S_{\text{BET}} = 1039 \text{ m}^2 \text{ g}^{-1}$; reaction time = 20 h) at room temperature, without the need for any heating, by introducing a minimum amount of NaOH.⁴⁰ However, to date, there have not been any reports demonstrating whether this route to CPO-27-Zn could afford similar or even higher STYs compared to that achieved in the hydrothermal synthesis of CPO-27-Ni, or whether it could be generalised to encompass CPO-27-M built up from metal ions other than Zn(II).

Seeking to further develop the aforementioned room-temperature, water-based chemistry, we have developed similar methods for several members of the CPO-27-M series, including ones made from Mg(II), Ni(II), Co(II), Cu(II) and Zn(II) ions. We optimised each method stepwise, by carefully studying the influence of reaction parameters on the purity and quality of the synthesised CPO-27-M and on the corresponding reaction yields. Specifically, we evaluated the pH, the reagent concentrations (of the metal acetate/nitrate [hereafter designed as *Met*] and of the dhtp), and the reaction time. We have proven that, except in the case of CPO-27-Cu, fine-tuning of these parameters for each CPO-27-M affords high-quality product (in terms of S_{BET}) with high STYs.

Experimental

Reagents

Nickel acetate tetrahydrate, cobalt acetate tetrahydrate, magnesium nitrate hexahydrate, zinc acetate dehydrate, copper acetate hydrate, 2,5-dihydroxyterephthalic acid (dhtp) and sodium hydroxide were purchased from Sigma Aldrich. Methanol was obtained from Fisher Chemical. All the reagents were used without further purification. Deionised water, obtained with a Milli-Q® system (18.2 MΩ·cm), was used in all reactions.

General protocol for the synthesis and activation of CPO- 27-M

Our protocol for the synthesis of CPO-27-M MOFs began with the addition of an aqueous solution of metal salt (*Met*) to an aqueous solution of dhtp and NaOH. The resulting reaction mixture, which contained the precursors *Met* (at the concentration C_1) and dhtp (at the concentration C_2), was stirred at room temperature for a certain period of time (t). In all cases, the volume was 10 mL and the molar ratio (*Met*/dhtp) was 2. After the time t , each resulting solid was collected by centrifugation, washed three times with water and methanol, dried at 70 °C overnight and weighed.

The prepared solids were characterised by XRPD, activated using a protocol recently described by Yaghi *et al.*,⁴¹ and their respective S_{BET} values were measured. The activation protocol started with the immersion of the synthesised CPO-27-M in methanol for 6 days (12 days for CPO-27-Mg), during which the solvent was exchanged once daily. Then, each CPO-27-M was exposed to five consecutive heating ramps under vacuum [from room temperature to 80 °C; from 80 °C to 100 °C; from 100 °C to 150 °C; from 150 °C to 200 °C, and from 200 °C to 250 °C (265 °C for CPO-27-Zn) at a constant rate of 4 °C min⁻¹, with the temperature held at 1 h at the end of each ramp; except for at 250 °C (265 °C for CPO-27-Zn), at which all samples were held for 12 h.

Gram-scale synthesis of CPO-27-Zn

In a typical synthesis, an aqueous solution of $\text{Zn}(\text{CH}_3\text{COO})_2 \cdot 2\text{H}_2\text{O}$ was rapidly added to an aqueous solution of dhtp and NaOH in a D15/CN10-F2 pilot-plant stirrer (DISPERMAT) equipped with a 1-L reactor. The volume of the reaction mixture was 500 mL; the molar ratio (*Met*/dhtp/NaOH/H₂O), 2:1:4:304; $C_1 = 0.365 \text{ mol L}^{-1}$; and $C_2 = 0.183 \text{ mol L}^{-1}$. This reaction mixture was stirred for 5 min at room temperature. The resulting solid was collected by centrifugation, washed three times with deionised water and methanol, and finally, dried at 70 °C overnight (weight: 32.5 g; yield: 97%).

Characterisation

X-ray powder diffraction (XRPD) patterns were collected on an X'Pert PRO MPDP analytical diffractometer (Panalytical) at 45 kV, 40 mA using CuK α radiation ($\lambda = 1.5419 \text{ \AA}$). Nitrogen adsorption and desorption measurements were done at 77K using an Autosorb-IQ-AG analyser (Quantachrome Instruments). Field-Emission Scanning Electron Microscopy (FE-SEM) images were collected on a FEI Magellan 400L scanning electron microscope at an acceleration voltage of 1.0-2.0 Kv, using aluminium as support. Transmission electron microscopy (TEM) images were obtained with a FEI Tecnai G² F20.

Results and discussion

Space-Time Yield (STY)

Space-Time Yield is an industrial parameter that refers to the quantity of a product (Kg) produced per unit volume (m^3) per unit time (day). Widely used in the field of catalysis,⁴² it has been employed by BASF to assess a given reaction/method for MOF production. Initial STY values reported by BASF include 60 $\text{Kg m}^{-3} \text{ day}^{-1}$ for the solvothermal synthesis of Basolite A100 (or MIL-53-Al), and 100 $\text{Kg m}^{-3} \text{ day}^{-1}$ and 225 $\text{Kg m}^{-3} \text{ day}^{-1}$ for the electrochemical synthesis of Basolite Z1200 (or ZIF-8) and Basolite C300 (or HKUST-1),⁴³ respectively.

Since the initial work of BASF, increasingly higher STYs have been reported for MOF synthesis. Interestingly, very competitive STYs have begun to be reported for water-based

Table 1. Summary of activation methods and S_{BET} values reported for CPO-27-M

CPO-27-M	Activation method	S_{BET} ($\text{m}^2 \text{g}^{-1}$)	References
Zn	Δ at a constant rate of 5°C min^{-1} from 25°C to 270°C , and then held at 270°C for 16 h	816	31
	Δ at a constant rate of 2°C min^{-1} from 25°C to 225°C , and then held at 265°C for 16 h	973	44
	Δ 10 h at 150°C , and then Δ 10 h at 265°C	496	22
	Δ 18 h at 350°C	867	45
	Δ 16 h at 100°C	948	46
	Δ 72 h at 100°C	885	27
	Not reported	1039	40
Ni	Δ at a constant rate of 5°C min^{-1} from 25°C to 250°C , and then held at 250°C for 5 h.	1070	31
	Δ at a constant rate of 2°C min^{-1} from 25°C to 225°C , and then held at 265°C for 16 h	1199	44
	Δ 5 h at 250°C	599	22
	Δ 18 h at 350°C	402	45
	Δ 16 h at 100°C	514	46
	Δ 19 h at 200°C , and then Δ 1 h at 110°C	1218	35
	Δ 20 h at 150°C	1233	38
	Δ 12 h at 250°C	1252	47
	Δ 6 h at 250°C	1350	26
	Δ 72 h at 100°C	1027	27
	Not reported	1018	24
	Not reported	1318	48
	Co	Δ at a constant rate of 5°C min^{-1} from 25°C to 250°C , and then held at 250°C for 5 h.	1080
Δ at a constant rate of 2°C min^{-1} from 25°C to 225°C , and then held at 265°C for 16 h		1292	44
Δ 24 h at 250°C		835	22
Δ 18 h at 350°C		521	45
Δ 16 h at 100°C		693	46
Δ 5 h at 250°C		1327	49
Δ 72 h at 100°C		1056	27
Not reported	1089	24	
Mg	Δ at a constant rate of 5°C min^{-1} from 25°C to 250°C , and then held at 250°C for 5 h.	1495	31
	Δ at a constant rate of 2°C min^{-1} from 25°C to 225°C , and then held at 265°C for 16 h	1530	44
	Δ 6 h at 250°C	1206	22
	Δ 18 h at 350°C	1007	45
	Δ 48 h at 240°C , and then Δ 1 h at 110°C .	1542	35
	Not reported	1415	24
	Δ 72 h at 100°C	1332	27
	Δ 12 h at 250°C	1416	47
	Δ 24 h at 250°C	1249	33
Δ 16 h at 250°C	877	50	

green syntheses of most iconic MOFs. Illustrative examples include a hydrothermal ($T = 60^\circ\text{C}$) synthesis of Basolite A520 (STY: $3600 \text{ Kg m}^{-3} \text{ day}^{-1}$) and a microwave ($T = 130^\circ\text{C}$) synthesis of Al fumarate (STY: $15200 \text{ Kg m}^{-3} \text{ day}^{-1}$), reported by BASF and Maurin, Serre *et al.*, respectively^{51, 52}. Impressive STYs have also been reported for the synthesis of HKUST-1 at room temperature ($2035 \text{ Kg m}^{-3} \text{ day}^{-1}$),⁵³ the hydrothermal ($T = 160^\circ\text{C}$) synthesis of MIL-100-Fe ($1700 \text{ Kg m}^{-3} \text{ day}^{-1}$ for),⁵⁴ the continuous flow hydrothermal ($T = 250^\circ\text{C}$) synthesis of MIL-53-Al ($1300 \text{ Kg m}^{-3} \text{ day}^{-1}$ for),¹² and the hydrothermal ($T = 100^\circ\text{C}$) synthesis of CPO-27-Ni ($680 \text{ Kg m}^{-3} \text{ day}^{-1}$).³⁸

Quality of a synthesised MOF

One parameter that is suitable for analysing the quality of a synthesised MOF is the surface area⁵⁵, which is generally reported as either the *BET surface area* (S_{BET}) or, less commonly, the *Langmuir surface area*. However, it is important to highlight here that S_{BET} is not a direct experimental value: it must be calculated from the N_2 isotherm

performed at 77 K according to the BET model. This fact, when considered together with the (variable) quality of the synthesised MOF and the activation method used, mean that the S_{BET} values reported for a particular MOF can vary widely. A clear example of a MOF for which various S_{BET} values have been reported is our target, CPO-27-M (Table 1). Another reason for the differences among reported S_{BET} values for a particular MOF is the pressure range selected for calculating the value. In order to enable comparison of different S_{BET} values for a given MOF, even when the MOF has been synthesised by different methodologies, the use of two criteria has recently been suggested:⁵⁵⁻⁵⁷ *firstly*, the straight line fitted to the BET plot must have a positive intercept; and *secondly*, the pressure range should be chosen such that $v_{\text{ads}}(1-P/P_0)$ always increases with P/P_0 . Accordingly, in the study reported here, we chose the pressure range based on these criteria.

As stated above, a second parameter that must be taken into account when comparing S_{BET} values is the activation process, which can also vary for a particular MOF. For instance,

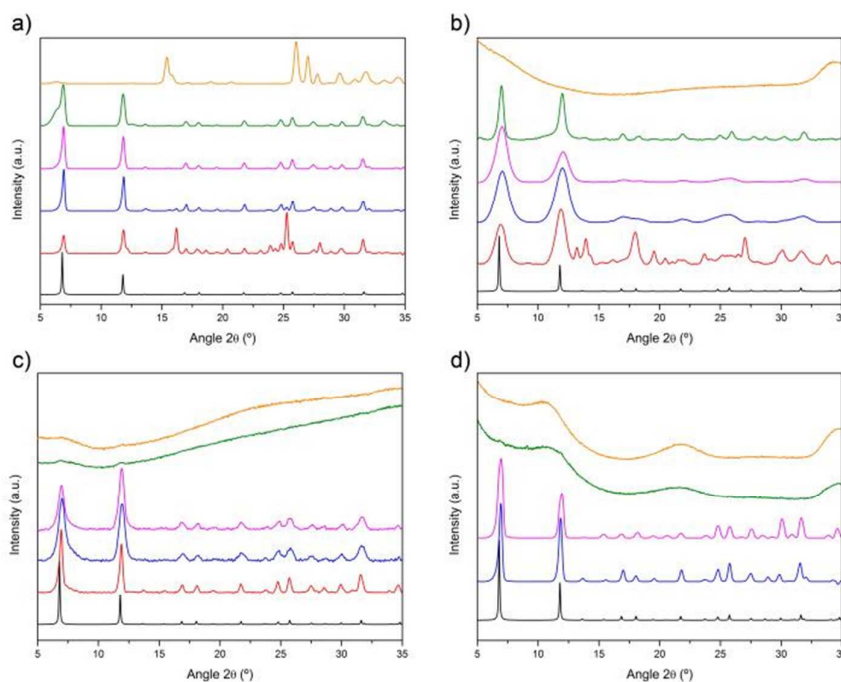


Fig. 1 XRPD diffractograms of the collected powder at different NaOH equivalents (Red: $x = 2$, Blue: $x = 3$, Pink: $x = 4$, Green: $x = 5$, orange: $x = 6$) for: a) CPO-27-Zn, b) CPO-27-Ni, c) CPO-27-Co and d) CPO-27-Mg, as compared to the simulated powder pattern for CPO-27 (black).

CPO-27-M has been activated by various methods (see Table 1). For consistency in the study reported here, we activated all the CPO-27-M samples using the general activation method described by Yaghi *et al.*⁵⁸

Optimisation of the room temperature water-based synthesis of CPO-27-M: STY versus quality

To increase the STY in a given MOF reaction, two parameters must be optimised: the *quantity of pure MOF produced per unit volume*, which must be maximised (mainly by balancing the maximum reaction yield and reagent concentrations); and the *reaction time*, which must be minimised. To optimise both parameters in our targeted syntheses of CPO-27-M, we followed a rational protocol comprising four steps. Firstly, we defined the maximum concentrations of Met (C_1) and dthp (C_2) that could be used. We found that the limiting concentration in the reaction mixture was $C_2 = 0.183 \text{ mol L}^{-1}$, which corresponds to the maximum amount of dthp that could be dissolved at room temperature under normal stirring conditions in 1 L of water in the presence of NaOH. By fixing the stoichiometry of metal ion and dthp in CPO-27-M (the total molar ratio of Met/dthp; to 2:1), C_1 and the total molar ratio Met/dthp/H₂O were then automatically defined to be 0.365 mol L^{-1} and 2:1:304, respectively. Secondly, we optimised the molar ratio of NaOH (hereafter designated as x) for the total molar ratio Met/dthp/H₂O = 2:1:304. For this, we studied the effect of the pH on the purity of the resulting CPO-27-M and on the reaction yields for a randomly selected reaction time of 24 h. At this point, we analysed the quality of the different CPO-27-M products synthesised at the optimum x by measuring their

S_{BET} . We considered CPO-27-M samples that showed S_{BET} values greater than 90% of the highest reported S_{BET} values (Table 1) to be of sufficiently high quality. Thirdly, those with lower S_{BET} values were optimised for quality, by decreasing C_1 and C_2 . Finally, once we had determined the ideal C_1 , C_2 and total molar ratio Met/dthp/NaOH (2:1:4) that afforded the maximum quantity of each CPO-27-M per volume unit with acceptable quality, we determined the lowest reaction time for each CPO-27-M, in order to achieve the highest STY.

Influence of the pH

We systematically studied a series of reactions that varied by total molar ratio (2:1: x :304, where $x = 2, 3, 4, 5$ and 6), in order to determine the optimum x in terms of purity and reaction yield. In the case of CPO-27-Zn, we found that an unidentified crystalline phase was formed at $x = 6$ (pH = 9.10); that a mixture of this amorphous phase and CPO-27-Zn was obtained at $x = 5$ (pH = 8.43); that pure CPO-27-Zn was synthesised at $x = 4$ (pH = 7.20), in a yield of 98%; and that a mixture of CPO-27-Zn and a second crystalline phase was obtained at $x = 2$ (pH = 6.27) and at $x = 3$ (pH = 6.86) (Fig. 1a). These results are in concordance with those observed by Sánchez-Sánchez *et al.*⁴⁰ At $x = 2$ and $x = 3$, we identified the second crystalline phase as $[\text{Zn}(\text{H}_2\text{O})_2(\text{dthp})]_n$,⁵⁹ in which only the two carboxylate groups—and not the two hydroxyl groups—of dthp are deprotonated and coordinate to Zn(II) ions (Fig. S1†). Interestingly, this coordination is quite different to that observed in CPO-27-Zn, in which the two hydroxyl groups of dthp are also deprotonated and coordinate to Zn(II) ions. Therefore, we reasoned that a minimum amount of NaOH is required to synthesise pure CPO-27-Zn, and that the

optimum amount should be $x = 4$, in order to fully deprotonate the carboxylate and hydroxyl groups of dhtp for their subsequent coordination to Zn(II) ions. To further prove this assumption, we also ran the reaction at $x = 3.25$, $x = 3.5$ and $x = 3.75$. Albeit pure CPO-27-Zn samples were produced, the reaction yields were lower (yields: 86%, 93% and 95%, respectively) compared to that obtained at $x = 4$ (yield: 98%).

We then extended the aforementioned systematic study to the other metal ions. Importantly, we found that $x = 4$ was also optimal for the water-based synthesis of CPO-27-Ni, CPO-27-Co and CPO-27-Mg at room temperature. However, the final products of the reactions in which x was altered, varied slightly depending on the metal ion. In the case of CPO-27-Ni, a second crystalline phase mixed with CPO-27-Ni was observed at $x = 2$ (pH = 5.92) (Fig. 1b). From $x = 3$ to $x = 5$, pure CPO-27-Ni samples were synthesised in yields of 62% ($x = 3$; pH = 6.77), 93% ($x = 4$; pH = 7.84) and 72% ($x = 5$; pH = 8.99). However, unidentified amorphous solid was formed at $x = 6$ (pH = 12.10). For CPO-27-Co, pure samples were synthesised in yields of 13% ($x = 2$; pH = 5.64), 55% ($x = 3$; pH = 5.96) and 98% ($x = 4$; pH = 8.03) (Fig. 1c). At $x = 5$ (pH = 10.04) and $x = 6$ (pH = 11.05), the precipitation of amorphous solids was observed. Finally, in the case of CPO-27-Mg, no precipitation occurred at $x = 2$ (pH = 4.61), whereas pure CPO-27-Mg samples were synthesised in yields of 48% ($x = 3$; pH = 8.08) and 91% ($x = 4$; pH = 9.18) (Fig. 1d). As with the cobalt MOF, amorphous solids were obtained at $x = 5$ (pH = 10.36) and $x = 6$ (pH = 11.95). Notice here that when the pH values are higher than 10, amorphous and unknown phases are formed in all cases. This observation is in concordance with the fact that these metal ions are not present as solvated ions above this pH, according to their Pourbaix diagrams.⁶⁰

Interestingly, we observed completely different behaviour for the reaction of dhtp with Cu(II) ions at the different x than that which we had observed for the other metals. We did not observe formation of CPO-27-Cu in any of the reactions, but we did observe an unknown phase that did not correspond to any reported phase resulting from the association of dhtp and Cu(II) ions (Fig. S2†). A potential explanation for such differences could be the trend of Cu(II) ions to form Cu(OH)₂ phases, even at pH < 7. Indeed, by comparing the Pourbaix diagrams of the different metal ions at a concentration of ~ 0.3 mol L⁻¹, one can observe that Ni(II), Zn(II), Mg(II) and Co(II) ions are stable as solvated ions until pH = 7, whereas Cu(II) ions show a higher tendency to form Cu(OH)₂ at this pH.⁶⁰

We then determined the S_{BET} values of the different CPO-27-M synthesised at the optimum NaOH concentration ($x = 4$), finding values of 900 m² g⁻¹ (CPO-27-Zn), 650 m² g⁻¹ (CPO-27-Ni), 1310 m² g⁻¹ (CPO-27-Co) and 1020 m² g⁻¹ (CPO-27-Mg). Based on these values, we determined that the CPO-27-Zn and CPO-27-Co were of sufficiently good quality and that sd their S_{BET} respective values fell above the 90 % of the maximum reported S_{BET} (Table 1).

Effect of the concentrations of the reagents

Having determined that the CPO-27-Ni and CPO-27-Mg products did not pass our quality threshold, we sought to find

the maximum concentration of reagents that would provide good quality S_{BET} in their respective syntheses. To this end, we decreased C_1 and C_2 . Thus, we systematically varied C_1 and C_2 (maintaining the molar ratio Met/dhtp/NaOH = 2:1:4; $C_1 = 0.273$ mol L⁻¹, 0.182 mol L⁻¹, 0.137 mol L⁻¹, 0.091 mol L⁻¹ and 0.069 mol L⁻¹) used in the synthesis of CPO-27-Ni and of CPO-27-Mg. Under the studied conditions, the highest C_1 and C_2 values that provided CPO-27-Ni (yield = 76%) with a good S_{BET} (1350 m² g⁻¹) were $C_1 = 0.069$ mol L⁻¹ and $C_2 = 0.0345$ mol L⁻¹. Note here that lower reagent concentrations led to a CPO-27-Ni that exhibited greater crystallinity and an enhanced S_{BET} (Table S1 and Fig. S3†). In the case of CPO-27-Mg, the optimal C_1 and C_2 were 0.273 mol L⁻¹ and 0.137 mol L⁻¹, respectively. Under these conditions, CPO-27-Mg, obtained in good yield (96%), exhibited an S_{BET} of 1337 m² g⁻¹ (Table S1 and Fig. S4†). However, in this case the use of lower reagent concentrations produced CPO-27-Mg of lesser crystallinity. We compared these results to those for CPO-27-Ni, and tentatively attributed the difference to the need for a critical concentration of dhtp to break the highly stable [Mg(H₂O)_x] complexes in water and form the MOF.

Influence of the reaction time

Once we had determined the highest C_1 and C_2 , we finally evaluated the minimum reaction time that enables synthesis of each CPO-27-M (Table S2†). For this, we performed a series of reactions decreasing the reaction times from 24 h to 5 min. For each reaction, we determined the yield and we characterised the resulting solids by XRPD and BET analysis. For all samples that passed our quality S_{BET} control threshold, we calculated the STY, taking into account the precursor concentrations, the yield and the reaction time (Table 2).

The minimum reaction times for CPO-27-Ni and -Mg were found to be 6 h and 4 h, respectively (Fig. S5,6†). At these times, the synthesised CPO-27-Ni showed a S_{BET} of 1220 m² g⁻¹ (yield = 92%), whereas CPO-27-Mg showed a S_{BET} of 1376 m² g⁻¹ (yield = 81%) (Fig. S9†). Taking into account these values, the STYs of these processes were 44 Kg m⁻³ day⁻¹ for CPO-27-Ni and 191 Kg m⁻³ day⁻¹ for CPO-27-Mg. Figure 2a,b shows representative Scanning Electron Microscopy (SEM) images for both materials, revealing the formation of CPO-27-Ni nanoparticles (mean size = 44 ± 7 nm) and hexagonal rod-like crystals of CPO-27-Mg (length = 1.1 ± 0.2 μm; width = 0.7 ± 0.1 μm). In the case of CPO-27-Co (Fig. S7†), the minimum reaction time was 1 h, which provided nanoparticles (mean size = 24 ± 5 nm) in 90% yield and with an S_{BET} of 962 m² g⁻¹ (Fig. 2c and S9†). The resulting STY of this reaction was 1462 Kg m⁻³ day⁻¹. Notice here that in the case of CPO-27-Ni and -Co nanoparticles, the use of a centrifugation step instead of a conventional filtration step may be required for collecting them. This limiting step should also be considered in a realistic industrial production using this room temperature water-based synthesis.

However, the most surprising result that we found was for CPO-27-Zn (Fig. S8†), which we were able to synthesise in only 5 min, in an excellent yield of 92% and with an S_{BET} of 1154 m²

Table 2. Comparison of the synthetic details, yield and S_{BET} values of CPO-27-M synthesised with the highest STY values and the highest S_{BET} values

CPO-27-M	C_1 (mol L ⁻¹)	C_2 (mol L ⁻¹)	Yield (%)	Time (h)	S_{BET} (m ² g ⁻¹)	V_p (cm ³ g ⁻¹) ^a	STY (kg m ⁻³ day ⁻¹)
Zn (mg scale)	0.364	0.182	92	0.08	1154	0.44	17986
Zn (g scale)	0.365	0.182	97	0.08	1076	0.40	18720
Zn	0.364	0.182	98	0.17	1279	0.47	9501
Co	0.364	0.182	90	1	962	0.39	1462
Co	0.045	0.023	93	24	1572	0.57	16
Mg	0.273	0.137	81	4	1376	0.52	191
Mg	0.182	0.091	94	6	1603	0.60	98
Ni	0.069	0.035	92	6	1220	0.48	44
Ni	0.069	0.036	76	24	1351	0.53	9

^a Pore volume was calculated at $P/P_0 = 0.15$ (N_2 , 77 K) using the Quantachrome ASiQWin software.

g⁻¹ (Fig. S9[†]). Under these conditions, the STY of the process was as high as 17986 Kg m⁻³ day⁻¹. Importantly, we also proved that this 5 min water-based synthesis of CPO-27-Zn is reproducible and can be synthesized at least to the gram scale (Fig. 2d,e). To scale up the reaction, we used the same conditions described above, except that we used larger quantities of each reagent (40.1 g Zn(Ac)₂; 18.1 g dhtp; 14.6 g NaOH; and 0.5 L H₂O) and a 1-L reactor. After only 5 min of reaction, 32.5 g (97% yield) of pure CPO-27-Zn ($S_{BET} = 1076$ m² g⁻¹) was collected (Fig. S10[†]). Based on these experimental conditions, the STY of this gram-scale process was 18720 kg m⁻³ day⁻¹. Fig. 2d,f shows SEM images for CPO-27-Zn synthesised at the milligram and gram scale, revealing the formation of hexagonal rod-like crystals in both cases. The length of CPO-27-Zn crystals synthesised at the gram scale (length = 9.3 ± 1.3 μm; width = 1.3 ± 0.3 μm) was slightly larger than those synthesised at the milligram scale (length = 5.5 ± 0.5 μm; width = 1.5 ± 0.6 μm). This difference is probably due to the sensitivity of the nucleation, and the crystal growth of CPO-27-Zn, to experimental factors such as the stirring homogeneity and rate.

Finally, the differences in the synthesis reaction rates of CPO-27-M materials [Zn(II) > Co (II) > Mg (II) > Ni (II)] may be explained as a result of the inertness or lability of the metal ions in the ligand exchange process. According with the water exchange rate constants of the complexes $[M(H_2O)_x]^{2+}$, the lability of the metal ions follows the order of Zn(II) > Co (II) > Mg (II) > Ni (II).⁶¹ As a consequence, the reaction rate between a highly labile $[Zn(H_2O)_x]^{2+}$ with a deprotonated ligand should be faster than the less labile $[Co(H_2O)_x]^{2+}$. In fact, these results are consistent with previous studies reported for the synthesis of CPO-27 materials under different reaction conditions, also showing that ligand exchange kinetics depends of the lability of the metals ions, being the determining step in the reaction between the deprotonated dhtp and the metal ions.^{62, 63}

Optimisation of the room temperature water-based synthesis of CPO-27-M in terms of BET surface area

Given that the conditions that provide an optimal STY do not generally deliver the best quality MOF, we further evaluated

the maximum achievable S_{BET} values for each CPO-27-M synthesised through the aforementioned reaction. By systematically modifying the same parameters (mainly, the precursor concentrations and the reaction time; Table 2), we ultimately observed that the S_{BET} values for CPO-27-Ni and CPO-27-Co increased with decreasing reagent concentrations and increasing reaction times. The best S_{BET} values were 1351 m² g⁻¹ for CPO-27-Ni (reaction time = 24 h; $C_1 = 0.069$ mol L⁻¹;

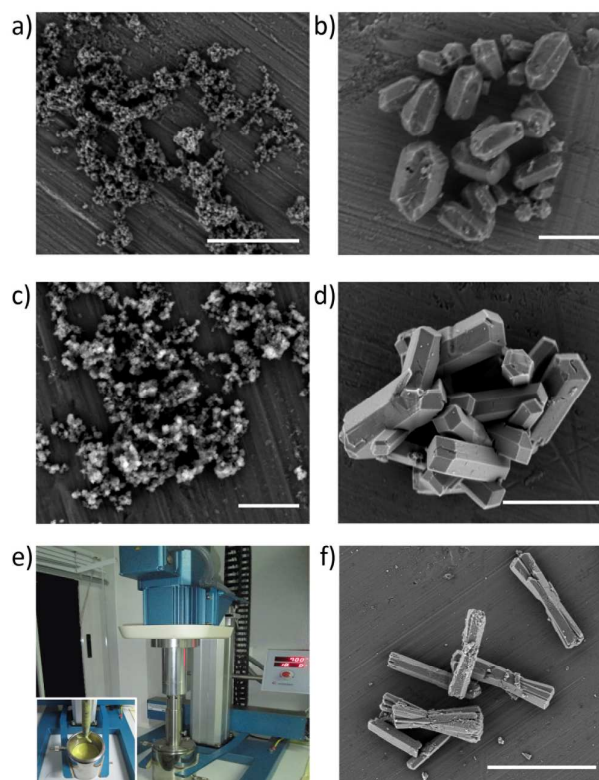


Fig. 2 Scanning Electron Microscope images of a) CPO-27-Ni, b) CPO-27-Mg, c) CPO-27-Co, d) CPO-27-Zn (mg-scale) and f) CPO-27-Zn (gram-scale) synthesized with the highest STYs. e) Pilot plant stirrer used in the scale-up synthesis of CPO-27-Zn. Scale bars: 1 μm (a, b, c) and 5 μm (d, f).

yield = 76%; STY = 9 Kg m⁻³ day⁻¹) and 1572 m² g⁻¹ for CPO-27-Co (reaction time = 24 h; C₁ = 0.045 mol L⁻¹; yield = 93%; STY = 16 Kg m⁻³ day⁻¹). On the contrary, the S_{BET} values for CPO-27-Zn and CPO-27-Mg increased with increasing precursor concentrations and decreasing reaction times. The maximum S_{BET} values were found to be 1279 m² g⁻¹ for CPO-27-Zn (reaction time = 10 min; C₁ = 0.364 mol L⁻¹; yield = 98%; STY = 9501 Kg m⁻³ day⁻¹) and 1603 m² g⁻¹ for CPO-27-Mg (reaction time = 6 h; C₁ = 0.182 mol L⁻¹; yield = 94%; STY = 98 Kg m⁻³ day⁻¹) (Fig. S11†). Interestingly, all these synthesised CPO-27-M crystals showed similar morphologies and sizes in comparison to those obtained for the highest STYs (Fig. S12†).

Conclusions

We have reported the stepwise optimisation of the room temperature, water-based synthesis of several members of the CPO-27/MOF-74-M series of MOFs, including ones made from Mg(II), Ni(II), Co(II) and Zn(II) ions. We evaluated the main reaction parameters affecting this method and found that by fine-tuning the pH, reagent concentrations and reaction time for each case, we were able to fabricate CPO-27-M with excellent BET surface areas (up to 1603 m² g⁻¹) and unprecedented STYs (as high as 18720 Kg m⁻³ day⁻¹). The development of such green syntheses, which obviate the use of costly and harmful organic solvents yet enable the efficient fabrication of high quality MOFs, should ultimately facilitate the industrial exploitation of these materials.

Acknowledgements

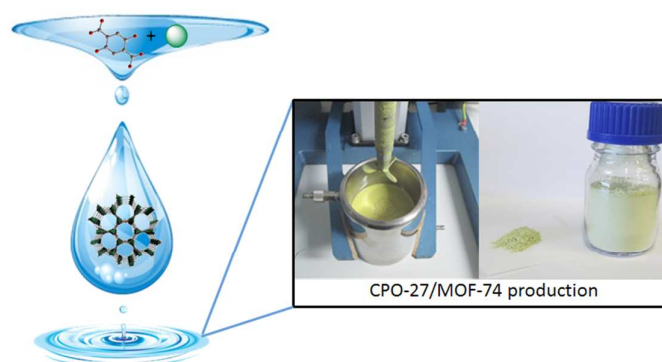
This work was supported by the Spanish MINECO (project PN MAT2012-30994) and the EC (project FP7 ERC-Co 61594). I.I. acknowledges the Spanish MINECO for a Ramón y Cajal grant. ICN2 acknowledges support of the Spanish MINECO through the Severo Ochoa Centres of Excellence Program (Grant SEV-2013-0295).

Notes and references

- Special issue on metal-organic framework materials. *Chem. Soc. Rev.* 2009, 1201.
- Special issue on metal-organic framework materials. *Chem. Soc. Rev.*, 43, 5403.
- H. Furukawa, N. Ko, Y. B. Go, N. Aratani, S. B. Choi, E. Choi, A. Ö. Yazaydin, R. Q. Snurr, M. O'Keeffe, J. Kim and O. M. Yaghi, *Science*, 2010, **329**, 424-428.
- P. Horcajada, R. Gref, T. Baati, P. K. Allan, G. Maurin, P. Couvreur, G. Férey, R. E. Morris and C. Serre, *Chem. Rev.*, 2012, **112**, 1232-1268.
- M. D. Allendorf and V. Stavila, *CrystEngComm*, 2015, **17**, 229-246.
- A. Carné, C. Carbonell, I. Imaz and D. Maspoch, *Chem. Soc. Rev.*, 2011, **40**, 291-305.
- N. Stock and S. Biswas, *Chem. Rev.*, 2012, **112**, 933-969.
- U. Mueller, M. Schubert, F. Teich, H. Puetter, K. Schierle-Arndt and J. Pastre, *J. Mater. Chem.*, 2006, **16**, 626-636.
- S. L. James, C. J. Adams, C. Bolm, D. Braga, P. Collier, T. Friscic, F. Grepioni, K. D. Harris, G. Hyett, W. Jones, A. Krebs, J. Mack, L. Maini, A. G. Orpen, I. P. Parkin, W. C. Shearouse, J. W. Steed and D. C. Waddell, *Chem. Soc. Rev.*, 2012, **41**, 413-447.
- A. Martinez Joaristi, J. Juan-Alcañiz, P. Serra-Crespo, F. Kapteijn and J. Gascon, *Cryst. Growth Des.*, 2012, **12**, 3489-3498.
- M. Rubio-Martinez, M. P. Batten, A. Polyzos, K.-C. Carey, J. I. Mardel, K.-S. Lim and M. R. Hill, *Sci. Rep.*, 2014, **4**.
- P. A. Bayliss, I. A. Ibarra, E. Perez, S. Yang, C. C. Tang, M. Poliakoff and M. Schroder, *Green Chem.*, 2014, **16**, 3796-3802.
- A. Carné-Sánchez, I. Imaz, M. Cano-Sarabia and D. Maspoch, *Nat Chem*, 2013, **5**, 203-211.
- M. Gaab, N. Trukhan, S. Maurer, R. Gummaraju and U. Müller, *Microporous Mesoporous Mater.*, 2012, **157**, 131-136.
- N. L. Rosi, J. Kim, M. Eddaoudi, B. Chen, M. O'Keeffe and O. M. Yaghi, *J. Am. Chem. Soc.*, 2005, **127**, 1504-1518.
- P. D. C. Dietzel, Y. Morita, R. Blom and H. Fjellvåg, *Angew. Chem. Int. Ed.*, 2005, **44**, 6354-6358.
- P. Valvekens, M. Vandichel, M. Waroquier, V. Van Speybroeck and D. De Vos, *J. Catal.*, 2014, **317**, 1-10.
- P. K. Allan, P. S. Wheatley, D. Aldous, M. I. Mohideen, C. Tang, J. A. Hriljac, I. L. Megson, K. W. Chapman, G. De Weireld, S. Vaesen and R. E. Morris, *Dalton Trans.*, 2012, **41**, 4060-4066.
- T. M. McDonald, J. A. Mason, X. Kong, E. D. Bloch, D. Gygi, A. Dani, V. Crocella, F. Giordanino, S. O. Odoh, W. S. Drisdell, B. Vlaisavljevich, A. L. Dzubak, R. Poloni, S. K. Schnell, N. Planas, K. Lee, T. Pascal, L. F. Wan, D. Prendergast, J. B. Neaton, B. Smit, J. B. Kortright, L. Gagliardi, S. Bordiga, J. A. Reimer and J. R. Long, *Nature*, 2015, **519**, 303-308.
- W. Zhou, H. Wu and T. Yildirim, *J. Am. Chem. Soc.*, 2008, **130**, 15268-15269.
- Z. Bao, S. Alnemrat, L. Yu, I. Vasiliev, Q. Ren, X. Lu and S. Deng, *Langmuir*, 2011, **27**, 13554-13562.
- T. Grant Glover, G. W. Peterson, B. J. Schindler, D. Britt and O. Yaghi, *Chem. Eng. Sci.*, 2011, **66**, 163-170.
- N. Wang, A. Mundstock, Y. Liu, A. Huang and J. Caro, *Chem. Eng. Sci.*, 2015, **124**, 27-36.
- L. Li, J. Yang, J. Li, Y. Chen and J. Li, *Microporous Mesoporous Mater.*, 2014, **198**, 236-246.
- M. H. Rosnes, M. Opitz, M. Frontzek, W. Lohstroh, J. P. Embs, P. A. Georgiev and P. D. C. Dietzel, *J. Mater. Chem. A*, 2015, **3**, 4827-4839.
- Y. Peng, V. Krungleviciute, I. Eryazici, J. T. Hupp, O. K. Farha and T. Yildirim, *J. Am. Chem. Soc.*, 2013, **135**, 11887-11894.
- H. Wu, W. Zhou and T. Yildirim, *J. Am. Chem. Soc.*, 2009, **131**, 4995-5000.
- K. Lee, J. D. Howe, L.-C. Lin, B. Smit and J. B. Neaton, *Chem. Mater.*, 2014.
- X. Kong, E. Scott, W. Ding, J. A. Mason, J. R. Long and J. A. Reimer, *J. Am. Chem. Soc.*, 2012, **134**, 14341-14344.
- D. Britt, H. Furukawa, B. Wang, T. G. Glover and O. M. Yaghi, *PNAS*, 2009, **106**, 20637-20640.
- S. R. Caskey, A. G. Wong-Foy and A. J. Matzger, *J. Am. Chem. Soc.*, 2008, **130**, 10870-10871.
- J. A. Mason, T. M. McDonald, T. H. Bae, J. E. Bachman, K. Sumida, J. J. Dutton, S. S. Kaye and J. R. Long, *J. Am. Chem. Soc.*, 2015, **137**, 4787-4803.
- T. Remy, S. A. Peter, S. Van der Perre, P. Valvekens, D. E. De Vos, G. V. Baron and J. F. M. Denayer, *The Journal of Physical Chemistry C*, 2013, **117**, 9301-9310.

34. J. Guasch, P. D. C. Dietzel, P. Collier and N. Acerbi, *Microporous Mesoporous Mater.*, 2015, **203**, 238-244.
35. P. D. C. Dietzel, V. Besikiotis and R. Blom, *J. Mater. Chem.*, 2009, **19**, 7362-7362.
36. P. D. C. Dietzel, Y. Morita, R. Blom and H. Fjellvåg, *Angew. Chem. Int. Ed.*, 2005, **44**, 6354-6358.
37. À. Ruyra, A. Yazdi, J. Espín, A. Carné-Sánchez, N. Röher, J. Lorenzo, I. Imaz and D. Maspoch, *Chem. Eur. J.*, 2015, **21**, 2508-2518.
38. S. Cadot, L. Veyre, D. Luneau, D. Farrusseng and E. Alessandra Quadrelli, *J. Mater. Chem. A*, 2014, **2**, 17757-17763.
39. D. J. Tranchemontagne, J. R. Hunt and O. M. Yaghi, *Tetrahedron*, 2008, **64**, 8553-8557.
40. M. Sanchez-Sanchez, N. Getachew, K. Diaz, M. Diaz-Garcia, Y. Chebude and I. Diaz, *Green Chem.*, 2015.
41. L. J. Wang, H. Deng, H. Furukawa, F. Gándara, K. E. Cordova, D. Peri and O. M. Yaghi, *Inorg. Chem.*, 2014, **53**, 5881-5883.
42. K. Weissermel and H.-J. Arpe, in *Industrial Organic Chemistry*, Wiley-VCH Verlag GmbH, 2007, pp. 424-438.
43. A. U. Czaja, N. Trukhan and U. Muller, *Chem. Soc. Rev.*, 2009, **38**, 1284-1293.
44. J. J. Perry, S. L. Teich-McGoldrick, S. T. Meek, J. A. Greathouse, M. Haranczyk and M. D. Allendorf, *The Journal of Physical Chemistry C*, 2014, **118**, 11685-11698.
45. M. Díaz-García, Á. Mayoral, I. Díaz and M. Sánchez-Sánchez, *Cryst. Growth Des.*, 2014, **14**, 2479-2487.
46. D. Ruano, M. Díaz-García, A. Alfayate and M. Sánchez-Sánchez, *ChemCatChem*, 2015, **7**, 674-681.
47. X. Wu, Z. Bao, B. Yuan, J. Wang, Y. Sun, H. Luo and S. Deng, *Microporous Mesoporous Mater.*, 2013, **180**, 114-122.
48. D.-J. Lee, Q. Li, H. Kim and K. Lee, *Microporous Mesoporous Mater.*, 2012, **163**, 169-177.
49. H.-Y. Cho, D.-A. Yang, J. Kim, S.-Y. Jeong and W.-S. Ahn, *Catal. Today*, 2012, **185**, 35-40.
50. P. D. C. Dietzel, R. Blom and H. Fjellvåg, *Eur. J. Inorg. Chem.*, 2008, **2008**, 3624-3632.
51. E. Leung, U. Müller, N. Trukhan, H. Mattenheimer, G. Cox and S. Blei, Patentanmeldung 10183283.0, 2010.
52. E. Alvarez, N. Guillou, C. Martineau, B. Bueken, B. Van de Voorde, C. Le Guillouzer, P. Fabry, F. Nouar, F. Taulelle, D. de Vos, J.-S. Chang, K. H. Cho, N. Ramsahye, T. Devic, M. Daturi, G. Maurin and C. Serre, *Angew. Chem. Int. Ed.*, 2015, n/a-n/a.
53. J. Huo, M. Brightwell, S. El Hankari, A. Garai and D. Bradshaw, *J. Mater. Chem. A*, 2013, **1**, 15220-15223.
54. Y.-K. Seo, J. W. Yoon, J. S. Lee, U. H. Lee, Y. K. Hwang, C.-H. Jun, P. Horcajada, C. Serre and J.-S. Chang, *Microporous Mesoporous Mater.*, 2012, **157**, 137-145.
55. T. Düren, F. Millange, G. Férey, K. S. Walton and R. Q. Snurr, *J. Phys. Chem. C*, 2007, **111**, 15350-15356.
56. J. Rouquerol, F. Rouquerol, P. Llewellyn, G. Maurin and K. S. W. Sing, *Adsorption by Powders and Porous Solids: Principles, Methodology and Applications*, Elsevier Science, 2013.
57. P. Llewellyn, F. R. Reinoso, J. Rouquerol and N. Seaton, *Characterization of Porous Solids VII: Proceedings of the 7th International Symposium on the Characterization of Porous Solids (COPS-VII), Aix-en-Provence, France, 26-28 May 2005*, Elsevier Science, 2006.
58. L. J. Wang, H. Deng, H. Furukawa, F. Gándara, K. E. Cordova, D. Peri and O. M. Yaghi, *Inorg. Chem.*, 2014, **53**, 5881-5883.
59. N. E. Ghermani, G. Morgant, J. d'Angelo, D. Desmaële, B. Fraisse, F. Bonhomme, E. Dichi and M. Sgahier, *Polyhedron*, 2007, **26**, 2880-2884.
60. G. Wulfsberg, *Principles of Descriptive Inorganic Chemistry*, University Science Books, 1991.
61. C. E. Housecroft and A. G. Sharpe, *Inorganic Chemistry*, Pearson Prentice Hall, 2012.
62. R. El Osta, M. Feyand, N. Stock, F. Millange and R. I. Walton, *Powder Diffr.*, 2013, **28**, S256-S275.
63. E. Haque and S. H. Jhung, *Chem. Eng. J.*, 2011, **173**, 866-872.

Table of contents



The stepwise optimisation of the room temperature, water-based synthesis of several porous CPO-27/MOF-74 materials allows fabricating them with BET surfaces areas up to $1603 \text{ m}^2 \text{ g}^{-1}$ and space-time-yields as high as $18720 \text{ Kg m}^{-3} \text{ day}^{-1}$.